# A rotationally invariant texture descriptor to detect copy move forgery in medical images

Surbhi Sharma
Dept. of Electronics and Communication Engineering
National Institute of Technology
Kurukshetra, India
s.surbhi1986@gmail.com

Umesh Ghanekar
Dept. of Electronics and Communication Engineering
National Institute of Technology
Kurukshetra, India
ugnitk@nitkkr.ac.in

***Abstract*— The wide spread use of multimedia communication and advancement in image processing techniques are the key factors that makes forgery easy. The copy-move is a very common forgery in digital images. Most of the techniques detect a copy move forgery of size less than 16×16. This paper, presents an efficient method to detect copy move forgery detection in medical images using center symmetric local binary pattern (CSLBP) which is able to detect the forgery size up to 12×12. The proposed block based method is robust against geometric distortion, gaussian blurring, JPEG compression and additive white gaussian noise. Simulation results exhibit that the proposed method outperforms many other well-known methods.**

***Keywords*— *Passive copy-move detection, medical image authentication, texture descriptor.***

## I. INTRODUCTION

Quotidian printed publications relays on digital images. With the advancement in image processing techniques, widespread use of internet, new developments in multimedia communication and the easiness in using image editing tools, the image contents can be easily changed when transferred electronically. The Digital image tampering detection is used in many fields like crime investigation, journalism, health insurance, surveillance systems, and also in medical imaging, where the images can be used as evidence. The managing editor of 'Journal of Cell Biology', estimated that 20% of the total accepted manuscripts to his journal have at least one tampered image and approximately 1% of diagrams are simply fraudulent [1]. Digital image tampering can be classified in two categories: a) Active techniques and b) Passive techniques. In active techniques [2-4], image authentication is done by comparing the received code and the sent code corresponding to the original Image. If both the codes are not same, then the image is tampered. In the medical field it is not possible to embed code at the time of image formation. Therefore, an alternative approach, i.e. passive image tampering detection [5-12] is used. In passive detection techniques, forgery is detected by finding the artifacts in the image produced by manipulative operations. The copy move attack is frequently used tampering, in which one or more than two regions are copied to the other parts of the same image. In early days, Discrete cosine transform (DCT) based technique was used to detect such type of image tampering [5]. Steganalysis based techniques such as Image Quality Matrics [6] and High Order Wavelet Statics [7] are used for medical images. Techebichef moments [8], spatial domain based [9] and transform based [10] are some other detection techniques used for passive image authentication.

All the techniques mentioned earlier having the limitation that they can detect the copy move paste area up to minimum size of 16×16 only. Also these techniques are not able to detect the forgery in presence of post processing operations. The proposed method is able to detect accurately up to minimum copy paste size of 12×12 even in the presence of gaussian blurring, additive white gaussian noise.

The paper is organized as follows. In Section II, we described the proposed detection scheme; Section III presents a number of experimental results that demonstrates the performance of the proposed scheme. Finally, Section IV provides the concluding remarks.

## II. PROPOSED METHOD

This section explains the proposed method for the detection of copy-move forgery in medical images. The proposed algorithm has three phases: preprocessing the input image, feature extraction and block matching.

### *A. Preprocessing phase*

The algorithm is developed for monochrome images only however, if the original image is RGB it can be converted into monochrome image using the following relationship:

$$Y = 0.299 \times R + 0.587 \times G + 0.114 \times B \tag{1}$$

As, the low frequency component of the images are more stable as compared to high frequency components. The low pass gaussian filter (w, σ) is used to extract low frequency components of the image.

### *B. Feature extraction phase*

The input image of size X×Y is divided into overlapping blocks of size B×B. Then using the sliding window method, we get number of overlapping blocks calculated as:

$$OV = \left(\left\lfloor\frac{X-B}{Separation}\right\rfloor + 1\right) \times \left(\left\lfloor\frac{Y-B}{Separation}\right\rfloor + 1\right) \tag{2}$$

978-1-4799-6023-1/15 $31.00 © 2015 IEEE
DOI 10.1109/CICT.2015.88

Separation denotes the pixel distance between two overlapping blocks. In the experiment, for feature extraction phase, we applied uniform rotational invariant $CSLBP_{N,R}$ to every block for getting features. Histogram of the uniform rotational invariant CSLBP codes is the required feature of the block. Feature of a block representing by a row in the feature matrix. CSLBP is a LBP variant proposed by [12] to obtain a shorter length LBP histogram and also to make LBP more stable against noise. The CSLBP of a pixel is calculated by comparing the center symmetric pairs of the surrounding of that pixel. The original LBP [11] produces $2^N$ binary patterns (N is the number of surrounding pixels), while the CSLBP produces only $2^{N/2}$ binary patterns. Suppose the reference pixel at position ($x_r$, $y_r$) having N number of equally spaced surrounding pixels placed at circumference of a circle with radius R. CSLBP is evaluated as below:

$$CSLBP(x_r, y_r) = \sum_{i=0}^{n/2-1} s(g_i - g_{(i+n/2)})2^i \;\; ; \;\; s(z) = \begin{cases} 1, & if \;\; z \geq 0 \\ 0, & Otherwise \end{cases} \qquad (3)$$

Where, the $g_i$ represents the gray value of neighbor pixels.

A texture descriptor used in passive forgery detection of copy move forgery should be rotationally invariant, so that if the copied region is rotated before pasting into the same image, it can still be detected. Rotational invariant CSLBP can be express by the Eq. (4):

$$CSLBP_{N,R}^{ri} = min\{ROR(CSLBP_{N,R}, i) | i == 0,1 \ldots\ldots N\} \qquad (4)$$

Where, function ROR (z, i) represents circular bitwise rotation of sequence z by i steps.

Natural images have many uniform areas like edges, spots, corners and flat areas which could be represented by a single pattern. An uniform CSLBP should have at most two bitwise transitions. Expression for the uniform rotation invariant CSLBP is given by Eq. (5):

$$CSLPB_{N,R}^{riu2} = \begin{cases} N+1 & Otherwise \\ \sum_{i=0}^{N-1} s(g_i - g_{\frac{i+n}{2}}) \;, & U(CSLBP_{N,R}) \leq 2 \end{cases} \qquad (5)$$

$U(CSLBP_{N,R})$ is the number of bitwise transitions.

*C. Block matching phase*

The Lexicographic sorting is used to get matching blocks. After row-sorted lexicographic, the matching rows become adjacent to each other in the matrix and corresponding blocks can be easily detected. But if the euclidean distance between the detected matched blocks is less than Dist, the proposed algorithm ignore them. The next is to calculate the shift vector between the remaining adjacent rows, corresponding to each shift vector, calculate shift vector counter. All the blocks which has shift vector counter greater than C are the desired copied moved block. Suppose ($x_1$,$y_1$) and ($x_2$,$y_2$) be the reference co-ordinates of two blocks which are represented by two consecutive rows of the sorted matrix .

$$S = (x_1 - x_2 \, , y_1 - y_2) \qquad (6)$$

The shift vector S between them is calculated by Eq.(6) . Normalize the shift vector so that S ≥ 0. For every pair of blocks corresponding to the consecutive rows of the sorted matrix, increment the shift counter C by one.

$$C(s_1, s_2) = C(s_1, s_2) + 1 \qquad (7)$$

Then the proposed method considers only those shift vectors $S_1$, $S_2$,… $S_k$ which has

$$C(S_r) \; > \; T_{shift} \quad ; \text{for } r=1,2,\ldots.k \qquad (8)$$

However, we assumed that the duplicated regions are not overlapping and the blocks are overlapping so shift vectors is counted if and only if the reference co ordinates of two matched blocks have euclidiean distance greater than dist: (9).

$$\sqrt{(x_1 - x_2)^2 + (y_1 - y_2)^2} \; > \text{dist} \qquad (9)$$

In summary, to get the matched blocks, two thresholds have to set: shift frequency threshold ($T_{shift}$) and euclidian distance threshold (dist). In the end, morphological opening is applied to fill the holes in the marked regions and to remove the isolated points.

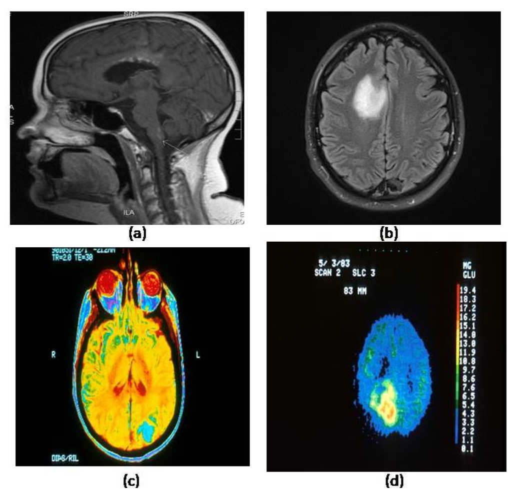


Fig. 1. Some original images used in the experiments.

## III. Experiment results

This section includes experimental setup and evaluation metrics. In the following section, the performance of the proposed algorithm is compared with other well known methods.

*A. Experimental setup*

The experiments were carried out on Dell laptop having intel core[i3] 2.40 GHz processor with Matlab 2012a. The two datasets [12-13] having different modalities images (CT, MRI, PET, X-RAYs) with different sizes and formats are being used. The tampered versions of source images were obtained using MATLAB. To evaluate the effectiveness of proposed method the following scenarios were considered: 1) simple copy move with different sizes 2) simple copy move and Additive White Gaussian Noise 3) Simple copy move and Gaussian Blurring 4) combined Transformations. In the experiment the parameters are set as B=10, dist=30, w=5, σ=0.5, N=8, R=1, $T_{SHIFT} \geq 5$.

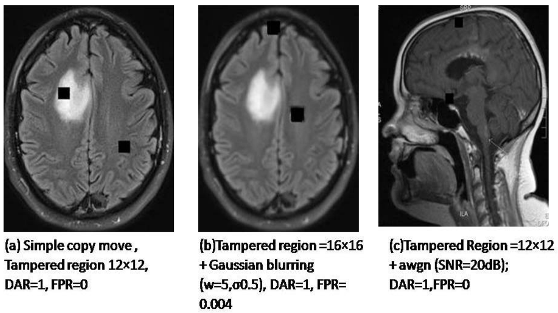


Fig. 2. Detection results for (a) Simple copy move, (b) gaussian blurring and copy move (c) awgn and copy move. Corresponding results are also showing in terms of DAR and FPR respectively.

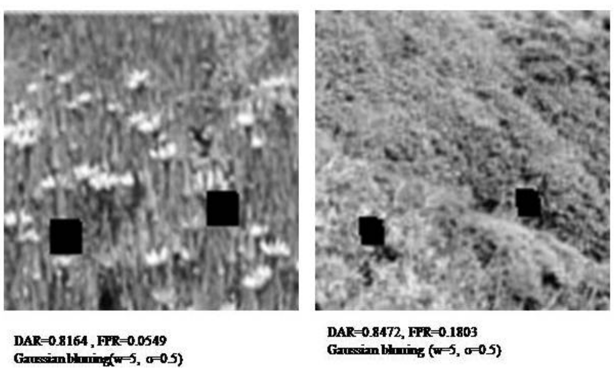


Fig. 3 Detection results on natural images.

## B. *Performance evaluation metrices*

The effectiveness of the Proposed method is evaluated in terms of Detection Accuracy Rate (DAR) and False Positive Rate (FPR) at pixel level. Expressions for these two quantitative measures are expressed by:

$$DAR = \frac{|\Omega_S \cap \widetilde{\Omega}_S| + |\Omega_T \cap \widetilde{\Omega}_T|}{|\Omega_S| + |\Omega_T|} \tag{10}$$

$$FPR = \frac{|\widetilde{\Omega}_S - \Omega_S| + |\widetilde{\Omega}_T - \Omega_T|}{|\widetilde{\Omega}_S| + |\Omega_T|} \tag{11}$$

Where, $\Omega_s$ and $\widetilde{\Omega}_s$ represents original copied and detected copied regions respectively. $\Omega_T$ and $\widetilde{\Omega}_T$ represents originally tampered and detected tampered region respectively.

## C. *Effectiveness and accuracy test*

Some of the color images and gray scale images with different modalities were selected from the two datasets. We categorized these images into three groups, consists of three different sized copy moved blocks which are 12×12, 16×16 and 32×32 respectively. Figure 1 is showing some original images used in the experiment and detection results are being shown in figure 2.

Table I. Comparison of detection efficiency of various techniques with 12×12 copy move tampered region.

| Tampered Region Size | **12*12** | | | | | |
|---|---|---|---|---|---|---|
| Modulity Type | Proposed | | DCT+SVD | | Fast copy | |
| | DAR | FPR | DAR | FPR | DAR | FPR |
| CT | 1 | 0 | CD | CD | CD | CD |
| MRI 1 | 1 | 0 | CD | CD | CD | CD |
| PET 1 | 1 | 0 | CD | CD | CD | CD |
| PET 2 | 1 | 0.10 | CD | CD | CD | CD |

#Note: CD=can't detect

## D. *Robustness test*

Forgers usually do some post processing operations such as additive gaussian noise, gaussian blurring, JPEG compression or mixed operation to create an imperceptible doctored image. Figure 2-3 shows that our algorithm can detect duplicated regions even under such post processing operations. However, literatures [9-10] do not give such results. The effectiveness of the proposed method over the previous methods such as [9-10] is represented by Tables I-V.

Table II. Comparison of detection efficiency of various techniques with 16×16 copy move tampered region.

| **Tampered Region Size** | **16*16** | | | | | |
|---|---|---|---|---|---|---|
| Modulity Type | Proposed | | DCT+SVD | | Fast copy | |
| | DAR | FPR | DAR | FPR | DAR | FPR |
| CT | 1 | 0 | 0.95 | 0.05 | 1 | 0 |
| MRI 1 | 1 | 0 | 1 | 0.891 | 1 | 0 |
| PET 2 | 1 | 0.05 | 1 | 0.889 | 0.2 | 2.8 |
| PET 3 | 1 | 0.062 | 1 | 0 | 1 | 0.9 |

Tables I-III indicates that when the tampered size is 16×16 or 32×32, the methods [9-10] works well but they failed to detect 12×12 tampered region. Only the CSLBP based method detected accurately. We can conclude from Table IV that the proposed method also did well in presence of gaussian blurring. In the presence of AWGN, the literature [9-10] performed well with 32×32 region but still was not able to detect 16×16 tampered region.

Table III. Comparison of detection efficiency of various techniques with 32×32 copy move tampered region.

| **Tampered Region Size** | **32*32** | | | | | |
|---|---|---|---|---|---|---|
| Modulity Type | Proposed | | DCT+SVD | | Fast copy | |
| | DAR | FPR | DAR | FPR | DAR | FPR |
| CT | 1 | 0.07 | 1 | 0 | 1 | 0 |
| MRI 1 | 1 | 0 | 1 | 0.673 | 1 | 0.6 |
| PET 2 | 1 | 0.02 | 1 | 0.005 | 1 | 0 |
| PET 3 | 1 | 0.014 | 1 | 0 | 1 | 0 |

Table IV. Comparison of detection efficiency of various techniques under the influence of gaussian blurring.

| **Tampered Region Size** | **16*16** | | | | | | | |
|---|---|---|---|---|---|---|---|---|
| Method | w=5,σ=0.5 | | w=5,σ=1 | | w=3,σ=0.5 | | w=3,σ=1 | |
| | DAR | FPR | DAR | FPR | DAR | FPR | DAR | FPR |
| Fast copy | CD | CD | CD | CD | CD | CD | CD | CD |
| DCT+ SVD | CD | CD | CD | CD | CD | CD | CD | CD |
| Proposed | 1 | 0.04 | 0.74 | 0 | 0.9 | 0.04 | 0.8 | 00 |

Table V. Comparison of detection efficiency of various techniques under the influence of AWGN.

| **Tampered Region Size** | **16*16** | | | | | |
|---|---|---|---|---|---|---|
| Method | SNR=30dB | | SNR=20dB | | SNR=15dB | |
| | DAR | FPR | DAR | FPR | DAR | FPR |
| Fast copy | CD | CD | CD | CD | CD | CD |
| DCT+SVD | 1 | 0.74 | 1 | 0.741 | 1 | 0.741 |
| Proposed | 1 | 0 | 1 | 0 | 1 | 0 |

## IV. Conclusion

This paper presents an efficient passive tampering detection of copy move for biomedical images. The efficacy of the proposed method is demonstrated by extensive simulations. The proposed method is able to identify the forged area up to 12×12 pixels under the influence of AWGN, gaussian blurring, where all other mentioned techniques fails to detect.

## References


[1] H. Pearson. Image manipulation: CSI: Cell biology. Nature, 434:952–953 ,2005.

[2] G. Coatrieux, H. Maitre, and B. Sankur, "Strict integrity control of biomedical images," in Proc. SPIE on SWMC III, pp. 229-240, 2001.

[3] X. Guo et T.-ge Zhuang, "Lossless Watermarking for Verifying the Integrity of Medical Images with Tamper Localization", Journal of Digital Imaging, vol. 22, no. 6, pp. 620-628, Dec. 2009.

[4] J.Tian, "Wavelet-based reversible watermarking for authentication", Proceedings of SPIE Photonics West, Security and Watermarking of Multimedia Contents, Vol. 4675-74, Pages 679-690, 2002.

[5] J. Fridrich, D. Soukal, J. Luka s, "Detection of copy-move forgery in digital images", Proceedings of Digital Forensic Research Workshops, Cleveland, OH, August, 2003.

[6] I.Avcıbas¸ N. Memon, and B. Sankur, "Steganalysis Using Image Quality Metrics," *IEEE Trans. on Image Processing*, vol. 12, pp. 221-229, February, 2003

[7] H. Farid, S. Lyu, "Higher-order Wavelet Statistics and their Application to Digital Forensics," Int. Conf. on Computer Vision and Pattern Recognition Workshop, vol. 8, pp. 94, 2003.

[8] H. Huang, G. Coatrieux, H.Z. Shu, L.M. Luo, Ch. Roux, "Blind Forensics in Medical Imaging Based on Tchebichef Image Moments", 33rd Annual International Conference of the IEEE EMBS, Boston, Massachusetts USA, August 30 - September 3, 2011.

[9] H.J Lin, C.W.Wang and Y.T kao, "Fast copy move forgery detection", WSEAS Transactions on Signal Processing, Issue 5, Volume 5,May 2009.

[10] J.Zhao and J. Guo, "Passive forensics for copy-move image forgery using a method based on DCT and SVD" , Forensic Science International 233, pp:158–166, 2013.

[11] T. Ojala, M. Pietikainen, and T. Maenpaa, "Multiresolution gray-scale and rotation invariant texture classificationwith local binary patterns," IEEE Transactions on Pattern Analysis and Machine Intelligence, vol. 24, no. 7, pp. 971–987, 2002.

[12] M. Heikkila, M. Pietikanen, C. Schmid, "Description of interest regions with local binary patterns", Pattern Recogn, vol 42, pp.425–36, 2009.

[13] www.visualonline.cancer.gov

[14] sun.aei.polsl.pl/~rstaros/**mednat**/index.html